Journal of Process Control 22 (2012) 1865–1877

Contents lists available at SciVerse ScienceDirect

Journal of Process Control

journal homepage: www.elsevier.com/locate/jprocont

RST controller design for a non-uniform multi-rate control system

A. Cuenca [a,*], J. Salt [b]

[a] Departamento de Ingeniería de Sistemas y Automática, Instituto Universitario de Automática e Informática Industrial, Universitat Politècnica de València, Spain
[b] Department of Mechanical Engineering. University of California at Berkeley USA

ARTICLE INFO

Article history:
Received 22 February 2012
Received in revised form 9 July 2012
Accepted 27 September 2012
Available online 25 October 2012

Keywords:
Non-uniform multi-rate controllers
RST controllers
LMIs

ABSTRACT

In this work, a non-uniform multi-rate controller which includes an RST control stage is introduced. Due to several issues, in some systems the use of non-uniform (irregular) multi-rate sampling becomes inevitable. When using a uniform (regular) multi-rate controller in this kind of situations, control performance is usually degraded (if it is compared to that obtained in the nominal, uniform sampling context). Thus, the design of a non-uniform controller proper for this sampling scheme is needed to keep the performance. A sequence of different non-uniform sampling frames can be considered, and different controllers must be designed for each frame using appropriate methods. When switching among these controllers, stability problems can appear. So, the control system stability will be assured in terms of Linear Matrix Inequalities (LMIs). To achieve some advantages at the design step, the discrete-time input–output representation will be used. But, since the classical, uniform z^{-i} delay operator could not be able to represent non-uniform sampling situations, the so-called non-uniform operator will be required. Simulation results illustrate that this control proposal is able to keep control system performance and preserve stability.

1. Introduction

There are some systems where the non-uniform (irregular) sampling appears in a natural way. It can be shown in hard disk drive head position control, where the location of damaged servo sectors and the collision in the self-servo track writing process make the feedback position error signal unavailable, resulting in a non-uniform sampling rate [1]; in real-time operating systems, where applications are implemented by decomposing them into several tasks in such a way that, due to task priorities and resource sharing, pre-emption and blocking may appear, arising irregularities in the sampling [2–4]; in networked control systems where sensors, controllers and actuators are connected through a common communication bus, which introduces timing variations in the control loop due to network induced delays, packet dropouts, and packet disordering [5–7]; in event-based systems where the sampling is triggered by the occurrence of some events, which usually appear following non-uniform patterns [8]; in many chemical processes, where variables which indicate product quality by means of chemical analyzers are infrequently and irregularly sampled [9–11]; and so on.

As a consequence of most of these sampling irregularities, control updates and output feedback measurements work at different rates. So, using multi-rate control techniques becomes a natural solution. In this work, feedback data is assumed to be scarce (which can be a realistic assumption in most of the previous environments). Then, a Multi-Rate Input Control (MRIC) scenario will be considered, where the control signal updating is faster than the output one (as known, actuating at a faster rate than measuring may provide robustness advantages [12]). But some restriction will be imposed to the MRIC approach: all the process inputs and outputs must be necessarily available at the slow rate time instants (that is, at the initial time of the sampling frame). This is not a hard restriction in most of the previous applications, except in networked control systems as a consequence of disposing no direct link among devices. Loss of packets, communication delays, etc. could appear, and hence all the samples could not be available at the required moments. In this particular case, some additional solutions can be adopted depending on the problem to be treated. For example, in [7] and [13] gain scheduling approaches were proposed to deal with delayed slow rate process inputs (that is, control actions). In [14], a non-uniform observer was introduced to estimate lost slow rate process outputs. These are two of the possible scenarios faced in previous authors' works, but other situations can be found in [5,6], and literature therein.

Whereas the uniform multi-rate sampling case has been widely studied (since the seminal work by Kranc [15] until current works such as [16–20]), the non-uniform case has been less treated (despite existing a lot of situations where it could be applied). To the best of the authors' knowledge, few research groups gather the majority of works that deal with this kind of sampling, where usually the non-uniform sampled-data system is represented as a

* Corresponding author. Tel.: +34 963877007; fax: +34 963879579.
E-mail addresses: acuenca@isa.upv.es (A. Cuenca), julian@isa.upv.es (J. Salt).

0959-1524/$ – see front matter © 2012 Elsevier Ltd. All rights reserved.
http://dx.doi.org/10.1016/j.jprocont.2012.09.010

Linear Periodically Time-Varying (LPTV) system. Refs. [1,3,21–23] are some examples of the referred works. Only in few of these works (such as [3,21]) the system is modeled by means of the input–output representation. Nevertheless, most of the works use the state–space representation, and more concretely, the well-known lifting technique to model and design the multi-rate control system. The main reason is because it facilitates the modeling step. Nevertheless, this technique introduces two main drawbacks at the design step: it could become more complex, and the consequent controller presents time-varying gains, which worsen the inter-sample behavior [24]. In the present work, these drawbacks are solved by using a specific algebra based on the so-called skip-expand operators [17,18,25]. As a consequence of using these operators, three benefits are derived:

The closed-loop system is not represented by an augmented lifted system, otherwise by a transfer function, which facilitates the design step.
When using the expand operator followed by a desired linear stationary filter (in our case a digital Zero Order Hold, ZOH), the slow-rate signal of the multi-rate control system can be approximated at a fast-rate signal, which enables to design the fast-rate side of the multi-rate controller.
When considering skip-expand properties, the multi-rate design complexity is reduced.

The non-uniform sampled-data modeling proposed in [3] is now revised, and its notation is improved and adapted to be used when designing the non-uniform multi-rate controller. The non-uniform modeling is based on the non-uniform operator, whose aim is to introduce some replacements on the uniform, classical operator z^{-i} in order to adapt the latter one to a non-uniform sampling pattern.

The multi-rate controller is designed via a model-based procedure. In [17] the multi-rate design for the uniform sampling case is introduced. In the present work, the non-uniform sampling scenario is studied and, in addition, an RST control stage is included in the multi-rate design. The RST controller is very popular due to its good compromise between performance and complexity. It is a two-degree-of-freedom controller obtained via an input–output model-based pole placement method, which implies the resolution of a diophantine equation. R–S–T is the names of each one of the polynomials to be deduced by the design procedure. Its two degree of freedom consists of a feedforward side defined by T/R, and of a feedback side defined by S/R. In [26], the general design procedure for the RST controller is introduced. In our work, this general method is adapted so as to include this controller in the multi-rate control system. The RST stage is designed to not cancel the numerator of the process transfer function. This fact, together with the use of the digital ZOH (commented previously), assures steady-state ripple-free closed-loop response to step reference signal [17,18]. Including the RST stage in the multi-rate controller simplifies the multi-rate control design. In [26], more details about this controller can be found.

An interesting benefit of the present work is the consideration of a sequence of different non-uniform sampling patterns (say, the non-periodic case). That means designing several LPTV controllers (one for each non-uniform sampling pattern) and switching among them according to the current frame. As known, it is possible to get instability by switching among asymptotically stable systems [27]. Then, to assure stability, some Lyapunov conditions will be formulated in terms of Linear Matrix Inequalities (LMIs).

The present paper is organized as follows: in Section 2 preliminaries and notation are introduced. The input/output modeling for non-uniform multi-rate sampled-data systems is reviewed. Its notation is improved and adapted to be used in the design proposal, yielding a theorem for the modeling step in Section 3. Section 4 presents another theorem, this one related to the design step, which describes how the RST control stage is included in the non-uniform multi-rate controller. Control system stability is studied from two points of view: sensitivity to modeling errors and stability for switching systems (which is enunciated in terms of LMIs). In Section 5, a simulation example is shown. Results enable to observe control performance degradation when using a (unique) uniform multi-rate controller in a non-periodic environment. Nevertheless, if different non-uniform multi-rate controllers (and the switching among them) are considered, the performance is kept (compared to a nominal, uniform sampling context) and stability preserved (according to the appropriate LMI analysis). Finally, in Section 6, the main conclusions are exposed.

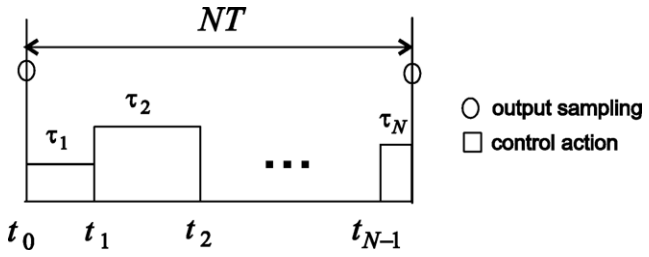

Fig. 1. MRIC scenario.

2. Preliminaries

Since notation used in [17,18] is becoming a standard fashion to represent multi-rate sampled-data systems, this work will take this notation to introduce preliminary concepts.

Two different Z-transforms can be expressed according to the considered sampling and updating periods over a continuous time signal $x(t)$. So, if the sampling or updating is carried out each T time units

$$X^T(z) \triangleq Z_T[x(t)] = \sum_{k=0}^{\infty} x(kT) z^{-k} \tag{1}$$

where X will be the sampled signal, and the variable z^{-1} represents the T-unit delay operator.

In the same way, if the sampling and updating period is NT ($N \in \aleph^+$)

$$X^{NT}(z_N) \triangleq Z_{NT}[x(t)] = \sum_{k=0}^{\infty} x(kNT) z_N^{-k} \tag{2}$$

where it is easy to see the relationship $z_N = z^N$.

In the MRIC scenario, the measurement period will be NT, which is usually called metaperiod. Inside this metaperiod, N control updatings are produced at time instants t_i ($i = 0 \ldots N-1$, where $t_0 = 0$), arising N subperiods τ_i ($i = 1 \ldots N$) among actuation instants (see Fig. 1). The relationship between samplings and subperiods yields

$$t_i = \sum_{j=1}^{i} \tau_j, \quad i = 1 \ldots N-1 \tag{3}$$

Two interesting operators are defined:

The skip operator, which is able to create a NT-sequence from a T-sequence, as follows:

$$\left[X^T(z)\right]^{NT} = X^{NT}(z_N) \triangleq \sum_{k=0}^{\infty} x(kNT) z^{-kN} \tag{4}$$

The expand operator, which creates a T-sequence from a NT-sequence, yielding

$$\left[X^{NT}(z_N)\right]^T = \hat{X}^T(z^N) \triangleq \sum_{k=0}^{\infty} \hat{x}(kT) z^{-kN} \begin{cases} \hat{x}(kT) = x(kT); & \forall k = \lambda N \\ \hat{x}(kT) = 0; & \forall k \neq \lambda N \end{cases} \quad \lambda \in Z^+ \tag{5}$$

Skip-expand properties can be found, for example, in [17,18,25].

Regarding an n-order single-input–single-output continuous time system represented by the strictly proper transfer function $G_p(s)$, its Fast Sampling Discrete-Time (FSDT) model is defined by

$$G^T(z) = \frac{B^T(z)}{A^T(z)} = \frac{\sum_{i=1}^{n} b_{i,T} z^{-i}}{1 + \sum_{i=1}^{n} a_{i,T} z^{-i}} \tag{6}$$

and, in a similar way, the Slow Sampling Discrete-Time (SSDT) model is defined as

$$G^{NT}(z_N) = \frac{B^{NT}(z_N)}{A^{NT}(z_N)} = \frac{\sum_{i=1}^{n} b_{i,NT} z^{-iN}}{1 + \sum_{i=1}^{n} a_{i,NT} z^{-iN}} \tag{7}$$

Finally, the Z-transform for $G_p(s)$ at a generic period t considering a Zero Order Hold (ZOH) device $H_t(s)$ will be used as

$$Z_t\left[H_t(s) G_p(s)\right] \triangleq G^t(\bar{z}) \tag{8}$$

3. Input/output non-uniform modeling for multi-rate sampled-data systems

In this section, a theorem which enunciates the input/output modeling for non-uniform sampled-data systems is presented. This theorem is defined after reviewing some previous results obtained in [3], and improving and adapting notation to that presented in Section 2.

3.1. Input/output uniform modeling

As known [17], the FSDT process $G^T(z)$ can be redefined by means of a polynomial $W_A^T(z)$, whose convolution with the polynomial $A^T(z)$ of the denominator produces a new denominator that contains only terms in $z^{-\lambda N}$ ($\lambda = 0, 1, \ldots, n$). Therefore:

$$G^T(z) = \frac{B^T(z)}{A^T(z)} = \frac{B^T(z) W_A^T(z)}{A^T(z) W_A^T(z)} = \frac{\tilde{B}^T(z)}{\left[A^{NT}(z_N)\right]^T(z)} \tag{9}$$

where

$$W_A^T(z) = \frac{\left[A^{NT}(z_N)\right]^T(z)}{A^T(z)} = \frac{\hat{A}^T(z_N)}{A^T(z)} = \prod_{k=1}^{N-1} A^T\left(z \cdot e^{\frac{-j2\pi k}{N}}\right) \tag{10}$$

From (9) and (10), the process can be modeled as a uniform sampled-data system [17]. To model the behavior of a non-uniformly sampled system the Z-transform can be also used, but some additional definitions are required. These ones are possible by introducing a suitable mathematical operator: the non-uniform operator $\sigma_N(i)$.

Definition: The non-uniform operator $\sigma_N(i)$ is defined by

$$\sigma_N(i) = \sum_{k=1}^{N} \frac{\exp\left(-s \sum_{l=k}^{i-1+k} \tau_l\right)}{N}, \quad i = 1 \ldots N-1 \tag{11}$$

where, as usual, s is referred to the Laplace variable.

Theorem (input/output non-uniform modeling): Given the FSDT process $G^T(z)$ in (6) and its polynomial $W_A^T(z)$ in (10), then $G^T(z)$ is modified by $W_A^T(z)$ resulting (9). If the first $N-1$ powers of the delay operator (i.e., z^{-i}, $i = 1 \ldots N-1$) in (9) are replaced by the non-uniform operator $\sigma_N(i)$ as follows:

- z^{-1} is replaced by

$$\sigma_N(1) = \left(\frac{e^{-s\tau_1} + e^{-s\tau_2} + \cdots + e^{-s\tau_N}}{N}\right) \tag{12}$$

- z^{-2} is replaced by

$$\sigma_N(2) = \left(\frac{e^{-s(\tau_1+\tau_2)} + e^{-s(\tau_2+\tau_3)} + \cdots + e^{-s(\tau_N+\tau_1)}}{N}\right) \tag{13}$$

- and so on, up to

$$z^{-(N-1)}. \tag{14}$$

Finally, z^{-N} is replaced by e^{-sNT}.

then $G^T(z)$ will be converted to $G_p^*(s)$ (where '*' means Laplace transform of the sampled system). After this conversion, two cases can be treated:

- uniform sampling ($\tau_i = \tau$): in this case some continuous zeros $\tilde{s} = -\tilde{\sigma} \pm j\tilde{w}_p$ are obtained, whose discretization at period T yields the discrete zeros included in $\tilde{B}^T(z)$.
- non-uniform sampling: here the continuous zeros change their location [28], being now in $\tilde{\tilde{s}} = -\tilde{\tilde{\sigma}} \pm j\tilde{\tilde{w}}_p$. Then, the model of the non-uniform sampled-data system will be defined as follows:

$$\tilde{\tilde{G}}^T(z) = \frac{\alpha \tilde{\tilde{B}}^T(z)}{\left[A^{NT}(z_N)\right]^T(z)} \tag{15}$$

where, by comparison with (9)

- $\tilde{\tilde{B}}^T(z)$ includes the new discrete zeros, which come from the appropriate discretization of the new continuous zeros $\tilde{\tilde{s}} = -\tilde{\tilde{\sigma}} \pm j\tilde{\tilde{w}}_p$. This discretization is carried out from this new period $\tilde{\tilde{T}}$:

$$\tilde{\tilde{T}} = \frac{\tilde{w}_p}{\tilde{\tilde{w}}_p} T \tag{16}$$

- α represents a suitable adjustment of the static gain

$$\alpha = \frac{\tilde{B}^T(1)}{\tilde{\tilde{B}}^T(1)} \tag{17}$$

- $\left[A^{NT}(z_N)\right]^T(z)$ includes the same discrete poles than in (9). Poles do not change their location under different sampling patterns [28].

In this way, despite using the z^{-i} delay operator, the non-uniform sampled-data system can be modeled as a LPTV system, where different τ_i can be considered inside the metaperiod NT.

Proof. Firstly, to determine the non-uniform operator $\sigma_N(i)$, a suitable study based on the frequency response of the process [28] is required (see details in Appendix I), leading to:

$$G_p^*(j\omega) = \frac{1}{NT} \sum_{i=0}^{N-1} G_i^{NT}\left(e^{jwNT}\right) \sum_{k=1}^{N} \exp\left(-jw \sum_{l=k}^{i-1+k} \tau_l\right) \tag{18}$$

where

- $z_N = z_N = e^{jwNT}$ (remember (1) and (2)),
- $G_i^{NT}\left(z^N\right) \triangleq \left[Z_{NT}\left[H_{NT}(s) G_p(s) e^{st_i}\right]\right]^T$, that is, the expanded Z-transform of the NT-period discretized impulse response, advanced t_i time instants and
- if $l > N$ then $\tau_l = \tau_{l-N}$.

If the expression (18) is enlarged, its first terms take the form

$$G_p^*(jw) = \frac{1}{T}\left[G_0^{NT}\left(e^{jwNT}\right) + G_1^{NT}\left(e^{jwNT}\right)\left(\frac{e^{-jw\tau_1} + e^{-jw\tau_2} + \cdots + e^{-jw\tau_N}}{N}\right) + G_2^{NT}\left(e^{jwNT}\right)\left(\frac{e^{-jw(\tau_1+\tau_2)} + e^{-jw(\tau_2+\tau_3)} + \cdots + e^{-jw(\tau_N+\tau_1)}}{N}\right) + \cdots\right] \tag{19}$$

From (19), the non-uniform operator $\sigma_N(i)$ can be defined by using the Laplace variable s (=jw) as follows:

$$\sigma_N(i) = \sum_{k=1}^{N} \frac{\exp\left(-s\sum_{l=k}^{i-1+k}\tau_l\right)}{N} \tag{20}$$

Then, applying (20) to (19), a well-known result can be obtained by drawing an analogy with [12]

$$G_p^*(s) \cong G_0^{NT}\left(e^{sNT}\right) + G_1^{NT}\left(e^{sNT}\right)\sigma_N(1) + G_2^{NT}\left(e^{sNT}\right)\sigma_N(2) + \cdots =$$

$$G_0^{NT}\left(e^{sNT}\right) + G_1^{NT}\left(e^{sNT}\right)\left(\frac{e^{-s\tau_1} + e^{-s\tau_2} + \cdots + e^{-s\tau_N}}{N}\right) \tag{21}$$

$$+G_2^{NT}\left(e^{sNT}\right)\left(\frac{e^{-s(\tau_1+\tau_2)} + e^{-s(\tau_2+\tau_3)} + \cdots + e^{-s(\tau_N+\tau_1)}}{N}\right) + \cdots$$

where $e^{sNT} \equiv z_N$ represents the sampling of the process each kNT, and the operator $\sigma_N(i)$ implies an effective sampling each $kNT - \sum_{x=i+1}^{N}\tau_x$, where $k = 0, 1, 2, \ldots$; $i = 1, 2, \ldots, N-1$.

In this way, from the process defined by (9), then the replacements (12)–(14) can be performed to obtain an expression like (21). And finally, taking into account (16) and (17), the input/output model for the non-uniform sampled-data system (15) can be achieved.

4. Non-uniform multi-rate control system design: stability analysis

4.1. RST controller design for a non-uniform multi-rate control system

In this section the classical RST controller [26] is adapted to be included in the multi-rate control system. As a consequence of this inclusion, the multi-rate controller design can be simplified. Fig. 2 shows a block diagram in order to easily appreciate how the control system is defined by two parts: a first side, where the RST control action is generated, and a second side that uses this action to calculate the non-uniform multi-rate control updating.

Assumption: As shown in Fig. 2, input and output samplers of the process work synchronized according to the non-uniform sampling pattern defined by τ_i. Then, the results are only valid under this assumption. However, this is not a very restrictive consideration, since at the process output only one of the N samples (the first one for each metaperiod) is later used by the controller, being the other ones, somehow, discarded from the point of view of the control system. Hence, τ_i can be selected according to the desired input (control) pattern.

4.1.1. RST controller

The RST controller [26] is a two-degree-of-freedom controller obtained via an input–output model-based pole placement design procedure, which implies the resolution of a diophantine equation. In this work (as shown in Fig. 2) to avoid confusion, the *RST* polynomials will be named as $\bar{R}\bar{S}\bar{T}$ (since R is used for the reference signal, and T for the sampling period). The polynomials $\bar{R}, \bar{S}$ are deduced when solving the diophantine equation. The polynomial $\bar{T}$ is designed to tune the control system gain, and to avoid unstable zero cancellations. The $\bar{R}\bar{S}\bar{T}$ control law in our proposal is designed at period NT, and yields

$$\bar{U}^{NT} = \frac{\bar{T}^{NT}(z_N)}{\bar{R}^{NT}(z_N)}R^{NT} - \frac{\bar{S}^{NT}(z_N)}{\bar{R}^{NT}(z_N)}\left[\tilde{\bar{Y}}_{DR}^{T}\right]^{NT} \tag{22}$$

The general procedure to obtain this law can be found in [26]. Next, a particular (but usual) case based on the consideration of a second order discrete-time process with a zero is detailed:

If the SSDT process model takes this form

$$G^{NT}(z_N) = \frac{k(z_N+b)}{(z_N-a_1)(z_N-a_2)} = \frac{k(z_N+b)}{(z_N^2+\alpha_1 z_N+\alpha_2)} = \frac{B^{NT}(z_N)}{A^{NT}(z_N)} \tag{23}$$

the SSDT reference model (including the zero of the process to avoid ripple problems) can be proposed as

$$M^{NT}(z_N) = \frac{(1+\bar{t}_1+\bar{t}_2)}{(1+b)}\frac{(z_N+b)}{(z_N^2+\bar{t}_1 z_N+\bar{t}_2)} = \frac{B_M^{NT}(z_N)}{A_M^{NT}(z_N)} = \frac{Y^{NT}(z_N)}{R^{NT}(z_N)} \tag{24}$$

Then, the pole placement approach yields the following diophantine equation

$$A^{NT}(z_N)\bar{R}^{NT}(z_N) + B^{NT}(z_N)\bar{S}^{NT}(z_N) = A_M^{NT}(z_N)A_o^{NT}(z_N) \tag{25}$$

where $A_o^{NT}(z_N)$ is the observer's polynomial (locating its poles usually in $z_N = 0$), and $\bar{R}, \bar{S}$ will take this form

$$\begin{aligned}\bar{R}^{NT}(z_N) &= (z_N + \bar{r}_1)\\ \bar{S}^{NT}(z_N) &= (\bar{s}_0 z_N + \bar{s}_1)\end{aligned} \tag{26}$$

So, solving the diophantine equation

$$\begin{aligned}\bar{s}_0 &= \frac{\bar{t}_1 - \alpha_1 - \bar{r}_1}{k}\\ \bar{s}_1 &= -\frac{\alpha_2\bar{r}_1}{kb}\\ \bar{r}_1 &= \frac{\bar{t}_2 - \alpha_2 + b\alpha_1 - b\bar{t}_1}{\alpha_1 - \frac{\alpha_2}{b} - b}\end{aligned} \tag{27}$$

being

$$\bar{T}^{NT}(z_N) = \frac{1+\bar{t}_1+\bar{t}_2}{k(1+b)}z_N \tag{28}$$

Remark 1. As known [26], disturbances are not used in the pole placement design. They can be indirectly included as constraints in the reference model, in the observer's polynomial, and in the control law.

4.1.2. Non-uniform multi-rate controller

Once the RST controller has been described, now the goal is to redefine the multi-rate controller in order to include the RST stage. As commented, the multi-rate controller will be designed via a model-based procedure [17]. The RST control stage will be included in the slow-rate side of the multi-rate controller, being obtained via an input–output model-based pole placement method [26] (as detailed in the previous section).

Theorem: Given a n-order single-input–single-output continuous-time process $G_p(s)$, whose closed-loop behavior

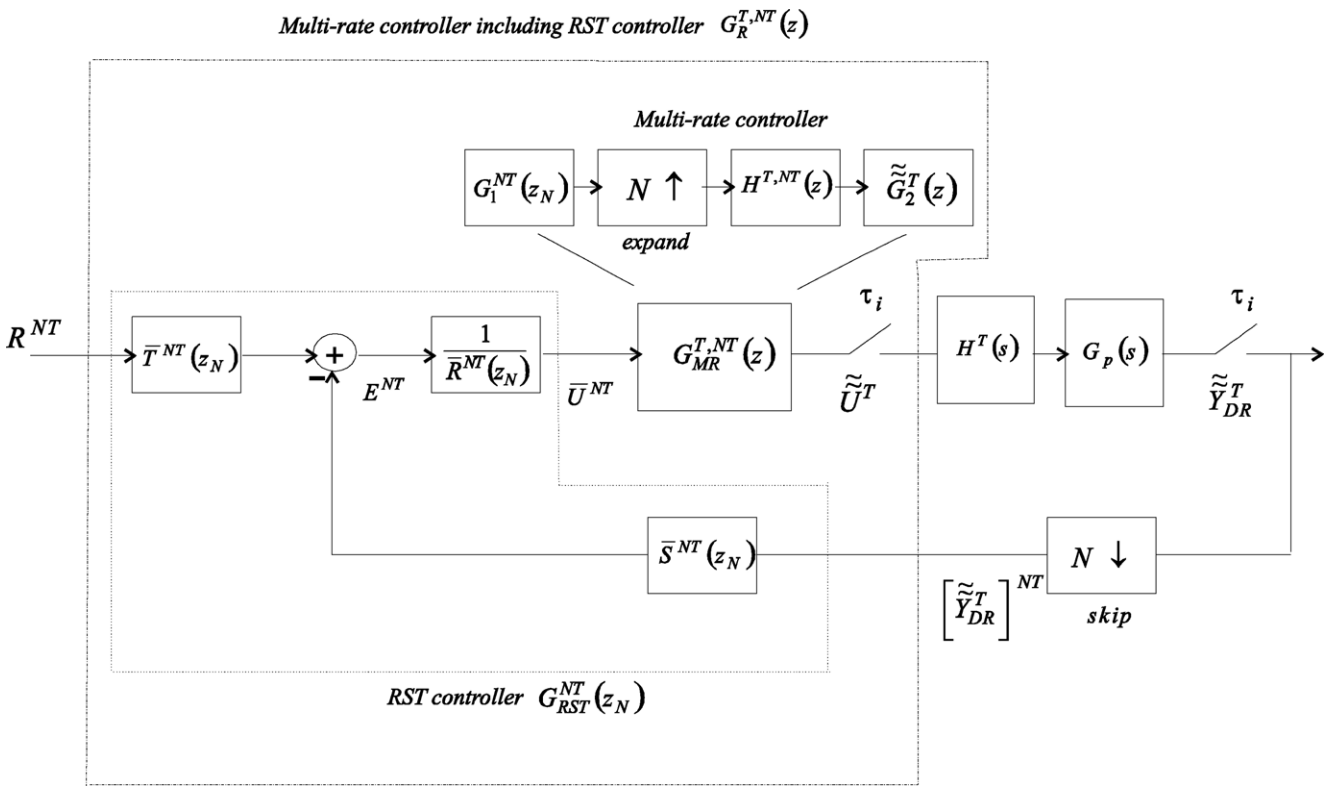

Fig. 2. Block diagram for the control system: multi-rate controller including an RST stage.

must follow the next continuous-time reference model $M(s)$, assuming a non-uniform control updating rate according to the subperiods τ_i, and the output being sampled at rate $1/NT$; if the skipped fast output $\left[\tilde{\tilde{Y}}_{DR}^T\right]^{NT}$ should match the slow single-rate control-loop output $Y^{NT}(z_N)$, that is, the slow-sampled output, then the controller should be

$$G_R^{T,NT}(z)=\frac{\alpha_M\tilde{\tilde{B}}_M^T(z)}{\alpha\tilde{\tilde{B}}^T(z)}\frac{R^T(z)}{\left[R^{NT}\right]^T(z)}\left[G_{RST}^{NT}(z_N)\frac{B^{NT}(z_N)}{B_M^{NT}(z_N)}\right]^T(z) \tag{29}$$

where

- $\tilde{\tilde{G}}_2^T(z)=\alpha_M\tilde{\tilde{B}}_M^T(z)/\alpha\tilde{\tilde{B}}^T(z)$ is the fast side of the multi-rate controller, being $\alpha_M\tilde{\tilde{B}}_M^T(z)$ the numerator of the FSDT reference model (since it is defined as $\tilde{\tilde{M}}^T(z)=\alpha_M\tilde{\tilde{B}}_M^T(z)/\left[A_M^{NT}\right]^T(z)$), and $\alpha\tilde{\tilde{B}}^T(z)$ the numerator of the FSDT process model (remember (15)),
- $G_1^{NT}(z_N)=B^{NT}(z_N)/B_M^{NT}(z_N)$ is the slow side of the multi-rate controller, where $B_M^{NT}(z_N)$ is the numerator of the SSDT reference model (remember (24)), and $B^{NT}(z_N)$ the numerator of the SSDT process model (remember (23)),
- $G_{RST}^{NT}(z_N)$ represents the RST controller, whose output is defined in (22),
- $H^{T,NT}(z)=\frac{R^T(z)}{\left[R^{NT}\right]^T(z)}$ is a rate converter located after the expanding block. It depends on the reference signal. So, for a step reference, it acts as a digital ZOH, then $H^{T,NT}(z)=(1-z^{-N})/(1-z^{-1})$.

Note that the expand operation is applied to the slow side of $G_R^{T,NT}(z)$, that is, $\left[G_{RST}^{NT}(z_N)G_1^{NT}(z_N)\right]^T(z)$ (remember Fig. 2).

For the particular case in which a uniform control updating at period T is considered, the controller should be

$$G_R^{T,NT}(z)=\frac{\tilde{B}_M^T(z)}{\tilde{B}^T(z)}\frac{R^T(z)}{\left[R^{NT}\right]^T(z)}\left[G_{RST}^{NT}(z_N)\frac{B^{NT}(z_N)}{B_M^{NT}(z_N)}\right]^T(z) \tag{30}$$

where only the fast side changes ($G_2^T(z)=\tilde{B}_M^T(z)/\tilde{B}^T(z)$), being $\tilde{B}_M^T(z)$ the numerator of the FSDT reference model (since it is defined in this case as $M^T(z)=\tilde{B}_M^T(z)/\left[A_M^{NT}\right]^T(z)$), and $\tilde{B}^T(z)$ the numerator of the FSDT process model (remember (9)).

Proof. From the well-known result about uniform multi-rate controllers (see "main result" pp. 992 in [17])

$$G_R^{T,NT}(z)=\frac{M^T(z)}{G^T(z)}\frac{R^T(z)}{\left[R^{NT}\right]^T(z)}\left[\frac{1}{1-M^{NT}(z_N)}\right]^T(z) \tag{31}$$

where

- $G_2^T(z)=M^T(z)/G^T(z)$ is the fast side of the multi-rate controller
- $\left[G_1^{NT}(z_N)\right]^T(z)=\left[1/(1-M^{NT}(z_N))\right]^T(z)$ is the expanded slow side of the multi-rate controller
- $H^{T,NT}(z)=R^T(z)/\left[R^{NT}\right]^T(z)$ is the rate converter located after the expanding block

If the SSDT reference model in (24) is redefined as

$$M^{NT}(z_N)=\frac{G_{RST}^{NT}(z_N)G^{NT}(z_N)}{1+G_{RST}^{NT}(z_N)G^{NT}(z_N)} \tag{32}$$

then the slow side of the multi-rate controller can be rewritten in this way

$$\frac{1}{1-M^{NT}(z_N)}=G_{RST}^{NT}(z_N)\frac{G^{NT}(z_N)}{M^{NT}(z_N)} \tag{33}$$

So, the multi-rate controller can be redefined as follows:

$$G_R^{T,NT}(z) = \frac{M^T(z)}{G^T(z)} \frac{R^T(z)}{\left[R^{NT}\right]^T(z)} \left[G_{RST}^{NT}(z_N) \frac{G^{NT}(z_N)}{M^{NT}(z_N)} \right]^T(z) \tag{34}$$

where

- $G_1^{NT}(z_N) = G^{NT}(z_N)/M^{NT}(z_N)$ is the new slow side of the multi-rate controller,
- $G_{RST}^{NT}(z_N)$ represents the RST controller, whose output is defined in (22).

Applying to the slow side $G_1^{NT}(z_N)$ both the expand operator (5) and the definition for $G^T(z)$ in (9), this slow side can be adapted in this way

$$\left[G_1^{NT}(z_N)\right]^T = \left[\frac{G^{NT}(z_N)}{M^{NT}(z_N)}\right]^T = \frac{\left[B^{NT}(z_N)\right]^T}{\left[A^{NT}(z_N)\right]^T} \frac{\left[A_M^{NT}(z_N)\right]^T}{\left[B_M^{NT}(z_N)\right]^T} = \frac{\left[B^{NT}(z_N)\right]^T}{\left[B_M^{NT}(z_N)\right]^T} \frac{A_M^T(z) W_{M_A}^T(z)}{A^T(z) W_A^T(z)} \tag{35}$$

In addition, using the non-uniform model (remember (15)), the fast side $\tilde{\tilde{G}}_2^T(z)$ can be represented by

$$\tilde{\tilde{G}}_2^T(z) = \frac{\tilde{\tilde{M}}^T(z)}{\tilde{\tilde{G}}^T(z)} = \frac{\alpha_M \tilde{\tilde{B}}_M^T(z)}{A_M^T(z) W_{M_A}^T(z)} \frac{A^T(z) W_A^T(z)}{\alpha \tilde{\tilde{B}}^T(z)} \tag{36}$$

So, as both sides of the multi-rate controller are now defined at the same period, they can be multiplied

$$\tilde{\tilde{G}}_2^T(z) \left[G_1^{NT}(z_N)\right]^T = \frac{\alpha_M \tilde{\tilde{B}}_M^T(z)}{A_M^T(z) W_{M_A}^T(z)} \frac{A^T(z) W_A^T(z)}{\alpha \tilde{\tilde{B}}^T(z)} \frac{\left[B^{NT}(z_N)\right]^T}{\left[B_M^{NT}(z_N)\right]^T} \times \frac{A_M^T(z) W_{M_A}^T(z)}{A^T(z) W_A^T(z)} = \frac{\alpha_M \tilde{\tilde{B}}_M^T(z)}{\alpha \tilde{\tilde{B}}^T(z)} \frac{\left[B^{NT}(z_N)\right]^T}{\left[B_M^{NT}(z_N)\right]^T} \tag{37}$$

Resulting

- $G_1^{NT}(z_N) = \frac{B^{NT}(z_N)}{B_M^{NT}(z_N)}$ (not including the expand operator)
- $\tilde{\tilde{G}}_2^T(z) = \frac{\alpha_M \tilde{\tilde{B}}_M^T(z)}{\alpha \tilde{\tilde{B}}^T(z)}$, or $G_2^T(z) = \frac{\tilde{B}_M^T(z)}{\tilde{B}^T(z)}$ (depending on the kind of sampling pattern)

Remark 2. $\tilde{\tilde{G}}_2^T(z)$ or $G_2^T(z)$ contains at denominator the numerator of the process model. Then, on the one hand, if this model is non-minimum phase, an unstable control signal will be generated. So, the proposed multi-rate controller is not appropriate for this case. In [29], the reader can find a suitable dual-rate controller for unstable and non-minimum phase systems. On the other hand, if the process is minimum phase, a safety region on the complex plain that includes some desired relative and absolute damping values can be defined. So, to avoid cancellation problems only those zeros of the model located inside this region will be cancelled [26].

Remark 3. The proposed multi-rate controller design only implies designing an RST controller at period *NT*, since both the slow and the fast sides are obtained from the corresponding modeling. It reduces highly the complexity of the design stage and the controller implementation.

4.2. Stability analysis

Once the control system is designed, now it is interesting to study its stability. So, two different stability aspects will be treated in this section. The first one is related to sensitivity to modeling errors. As known, mismatches between model and process can imply some degradation of the control system performance and stability. Theorem 5.4 in [26] is particularized to our case in order to introduce some upper-bounded condition to evaluate the control system stability in the presence of these mismatches.

The second aspect to be faced will be stability for switching systems. In the previous section, the design of a non-uniform multi-rate control system which includes an RST control stage is studied. As a result, the control system can be represented as a LPTV system. But, as commented, in some environments can appear different non-uniform patterns (the non-periodic case). So, different LPTV control systems must be designed in order to switch among them according to the current pattern. Although each one of the consequent LPTV control systems was stable, the switching among them could imply instability. In this work, in order to assure stability for the switching case, a LMI analysis will be carried out. This analysis requires the closed-loop system at *NT*-period, since, as well-known (see for example in [12]), any LPTV system is globally defined at metaperiod *NT*.

Lemma: From the notation depicted in Fig. 2, the multi-rate closed-loop system at *NT*-period is defined as

$$\frac{\left[\tilde{\tilde{Y}}_{DR}^T\right]^{NT}}{R^{NT}}(z_N) = \frac{\left[\tilde{\tilde{G}}^T \tilde{\tilde{G}}_2^T H^{T,NT}\right]^{NT} G_1^{NT}(\bar{T}^{NT}/\bar{R}^{NT})}{1 + \left[\tilde{\tilde{G}}^T \tilde{\tilde{G}}_2^T H^{T,NT}\right]^{NT} G_1^{NT}(\bar{S}^{NT}/\bar{R}^{NT})}(z_N) \tag{38}$$

Note that in a uniform case $G^T(z)$ and $G_2^T(z)$ will be used instead of $\tilde{\tilde{G}}^T(z)$ and $\tilde{\tilde{G}}_2^T(z)$, respectively.

Proof. From [17], if the RST controller is considered, the process output for the non-uniform multi-rate controlled system will fulfill

$$\tilde{\tilde{Y}}_{DR}^T(z) = \tilde{\tilde{G}}^T \tilde{\tilde{G}}_2^T H^{T,NT} \left[G_1^{NT}\right]^T \left[\frac{\bar{T}^{NT}}{\bar{R}^{NT}} R^{NT} - \frac{\bar{S}^{NT}}{\bar{R}^{NT}} \left[\tilde{\tilde{Y}}_{DR}^T\right]^{NT}\right]^T(z) \tag{39}$$

If this output is skipped, and assuming the skip-expand properties in [17,25]

$$\left[\tilde{\tilde{Y}}_{DR}^T\right]^{NT}(z_N) = \left[\tilde{\tilde{G}}^T \tilde{\tilde{G}}_2^T H^{T,NT} \left[G_1^{NT}\right]^T \left[\frac{\bar{T}^{NT}}{\bar{R}^{NT}} R^{NT} - \frac{\bar{S}^{NT}}{\bar{R}^{NT}} \left[\tilde{\tilde{Y}}_{DR}^T\right]^{NT}\right]^T\right]^{NT} = \left[\tilde{\tilde{G}}^T \tilde{\tilde{G}}_2^T H^{T,NT}\right]^{NT} G_1^{NT} \left[\frac{\bar{T}^{NT}}{\bar{R}^{NT}} R^{NT} - \frac{\bar{S}^{NT}}{\bar{R}^{NT}} \left[\tilde{\tilde{Y}}_{DR}^T\right]^{NT}\right](z_N) \tag{40}$$

(39) is obtained.

Control system sensitivity to modeling errors: When obtaining $\tilde{\tilde{G}}^T(z)$ (or $G^T(z)$), some modeling errors could be made, resulting differences between the model $\tilde{\tilde{G}}^T(z)$ and the real process $\tilde{\tilde{G}}_0^T(z)$. This fact usually implies some degradation on the control system performance and stability. Focusing on stability, from Theorem 5.4 in [26] the mismatch between process and model is upper-bounded according to the next well-known condition (Eq. (5.11) in [26], now particularized to our case):

$$\left|H_{lg}^{NT}(z_N) - H_{lg,0}^{NT}(z_N)\right| < \left|1 + H_{lg}^{NT}(z_N)\right| \tag{41}$$

where, remembering (38):

- $H_{lg}^{NT}(z_N) = \left[\tilde{\tilde{G}}^T \tilde{\tilde{G}}_2^T H^{T,NT}\right]^{NT} G_1^{NT}(\bar{S}^{NT}/\bar{R}^{NT})(z_N)$ is the loop gain when the model $\tilde{\tilde{G}}^T(z)$ is considered.

– $H_{lg,0}^{NT}(z_N) = \left[\tilde{\tilde{G}}_0^T \tilde{\tilde{G}}_2^T H^{T,NT}\right]^{NT} G_1^{NT}(\bar{S}^{NT}/\bar{R}^{NT})(z_N)$ is the loop gain when the real process $\tilde{\tilde{G}}_0^T(z)$ is considered.

From (41), despite the presence of mismatches, the closed-loop stability referred to $\tilde{\tilde{G}}_0^T(z)$ is assured for $|z_N| = 1$ (as indicated by theorem 5.4 in [26]). Since, $z_N = e^{sNT}\big|_{s=jw} = \cos(wNT) + j\sin(wNT)$, and $|z_N| = \sqrt{\cos^2(wNT) + \sin^2(wNT)} = 1$, then (41) must be evaluated for $z_N = 1$ (that is, $w = 0$), and $z_N = -1$ (that is, $w = \pi/NT$).

Remark 4. Since skip operations are included in (41), this expression is evaluated at period NT. Thus, no noticeable differences should be yielded when (41) is checked for the uniform model $G^T(z)$ with respect to when it is checked for the non-uniform model $\tilde{\tilde{G}}^T(z)$. Both models present the same behavior at period NT.

Switching system stability: Let us convert (38) into state–space representation, in such a way that the closed-loop matrix A_{cl} includes the eigenvalues of the LPTV system. But these eigenvalues will vary according to the non-uniform pattern considered in each metaperiod, that is, A_{cl} depends on a set of parameters $\rho_k = \{\tau_{1,k}, \tau_{2,k}, \ldots, \tau_{N-1,k}\}$, which includes the subperiods τ_i between two consecutive time instants where the control updating is produced for each metaperiod kNT. So, A_{cl} will be replaced by $A_{cl}(\rho_k)$ to express the non-periodicity feature of the system, and the closed-loop system will be defined as

$$x[(k+1)NT] \equiv x_{k+1} = A_{cl}(\rho_k)x_k \tag{42}$$

In this work, a geometric decay rate $0 \le \alpha \le 1$ will be used in order to prove the stability condition. So, the next common Lyapunov function

$$V(x) = x^T Q x, \quad Q > 0 \tag{43}$$

must be found [30] so that $V[(k+1)NT] < \alpha^2 V[kNT]$. Replacing (42) in (43), the Lyapunov decrescence conditions can be written as the following matrix inequality:

$$A_{cl}(\vartheta)^T Q A_{cl}(\vartheta) - \alpha^2 Q < 0, \quad \forall \vartheta \in \theta \tag{44}$$

where ϑ is a dummy parameter ranging in a set θ where the non-periodic parameters ρ_k are assumed to take values in, and matrix Q is composed of decision variables to be found by the semidefinite programming solver.

If $A_{cl}(\rho_k)$ is an affine function of ρ_k, and θ is polytopic, then (44) can be checked with a finite number of LMIs. Otherwise, a LMI gridding procedure [31] must be used to approximately check for the above conditions. In [13] a stochastic approach for this LMI procedure can be found.

Control system modeling and design procedure: Finally, to complete this Section 4, a schematic procedure which sorts out the modeling and design steps to be followed is presented.

– Step 1: From $G_p(s)$, obtain the FSDT model for the uniform case $G^T(z)$ (by (9)) and for the non-uniform cases $\tilde{\tilde{G}}^T(z)$ (by (15), considering one model for each sampling pattern), and the SSDT model $G^{NT}(z_N)$ (by (7)).
– Step 2: Define a reference model $M(s)$ and obtain the consequent FSDT model for the uniform case $M^T(z)$ (defined after (30)) and for the non-uniform cases $\tilde{\tilde{M}}^T(z)$ (defined after (29), obtaining one model for each sampling pattern), and the SSDT model $G^{NT}(z_N)$ (by (24)).
– Step 3: Design the RST control stage by solving the diophantine equation in (25). So, the RST polynomials in (26), (28) are obtained, and hence the control law in (22) can be stated.
– Step 4: Design the multi-rate controller according to (30) for the uniform case, and (29) for each non-uniform case.
– Step 5: Assure stability in term of LMIs (44) for the case in which switching among non-uniform controllers is considered. Check the condition (41) to evaluate sensitivity to modeling errors.
– Step 6: Use suitable performance indexes in order to compare the behavior of each designed control system.

5. Simulation example

One of the aims of this example is to show how, when a process is sampled in a non-uniform way, an accurate model for it can be reached following the steps provided by theorem of Section 3. Despite its reliability, sensitivity to modeling errors will be studied too.

Another goal of the example is to compare three different situations. The first of them is the uniform sampling case. In this context a uniform multi-rate controller is designed in order to achieve some performance (the nominal one). If this controller is used when a non-uniform sampling pattern appears, the performance will be degraded. Thus, a non-uniform multi-rate controller will be designed to keep the nominal control performance. In addition, if a sequence of different non-uniform patterns appears, a set of non-uniform controllers must be designed in order to switch among them according to the current pattern. With this strategy the performance can be kept, whereas if a unique uniform multi-rate controller is used, the performance becomes worst. This study will be developed by simulating control system outputs and by checking stability via LMIs.

5.1. Modeling steps

Given a continuous time process $G(s) = (s+3)/(s^2+2s+2)$, which presents a settling time around 4 s ($t_s = 4$ s), if an output sampling period $NT = 0.6$ s (with $N = 2$) is considered, its SSDT and uniform FSDT models are, respectively, defined by

$$G^{NT}(z_N) = \frac{0.6656(z_2 - 0.1092)}{z_2^2 - 0.9059z_2 + 0.3012} = \frac{B^{NT}(z_N)}{A^{NT}(z_N)} \tag{45}$$

$$G^T(z) = \frac{0.3289(z - 0.3919)}{z^2 - 1.415z + 0.5488} = \frac{B^T(z)}{A^T(z)} \tag{46}$$

being $W_A^T(z) = z^2 + 1.415z + 0.5488$.

Two different non-uniform patterns $\{\tau_1, \tau_2\}$ will be considered: $\{0.45, 0.15\}$ (that is, sampling at [0, 0.45] time instants for each metaperiod) and $\{0.55, 0.05\}$ (that is, sampling at [0, 0.55] time instants for each metaperiod). The consequent non-uniform FSDT process models take this form (after applying the modeling introduced in Section 3)

$$\text{for } \{0.45, 0.15\}: \tilde{\tilde{G}}^T(z) = \frac{0.4877(z - 0.3945)\left(z^2 + 0.7542z + 0.2537\right)}{z^4 - 0.9059z^2 + 0.3012} = \frac{\alpha\tilde{\tilde{B}}^T(z)}{\left[A^{NT}\right]^T(z)} \tag{47}$$

$$\text{for } \{0.55, 0.05\}: \tilde{\tilde{G}}^T(z) = \frac{0.6144(z - 0.3795)\left(z^2 + 0.4630z + 0.0920\right)}{z^4 - 0.9059z^2 + 0.3012} = \frac{\alpha\tilde{\tilde{B}}^T(z)}{\left[A^{NT}\right]^T(z)} \tag{48}$$

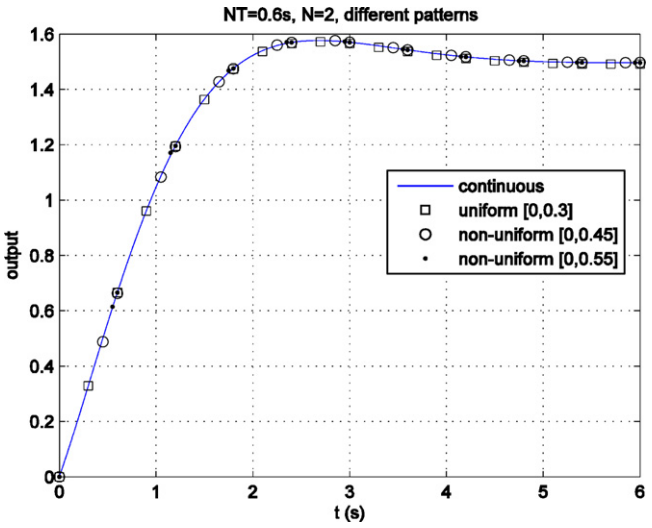

Fig. 3. Process outputs for different patterns.

Fig. 3 depicts the sequence of process output values which is provided by each non-uniform model for a step reference. In addition, the uniform case and the continuous output are also shown. The sampled values are located at the correct continuous output response according to each sampling pattern. As expected, the first value of each metaperiod (every $NT = 0.6$ s) coincides for all sampling patterns.

In this example the goal of the design procedure is to achieve some improvement in the settling time in such a way that it can be reduced around 50% ($t_s = 2$ s). So, the next reference model is considered $M(s) = (s+3)/(s^2+4s+8)$, being its SSDT and FSDT transfer functions:

$$M^{NT}(z_N) = \frac{0.3692(z_2 - 0.1138)}{z_2^2 - 0.2183z_2 + 0.09072} = \frac{B_M^{NT}(z_N)}{A_M^{NT}(z_N)} \tag{49}$$

$$M^{T}(z) = \frac{0.2439(z - 0.3922)}{z^2 - 0.9059z + 0.3012} = \frac{B_M^{T}(z)}{A_M^{T}(z)} \tag{50}$$

where $W_{M_A}^T(z) = z^2 + 0.9059z + 0.3012$.

For the non-uniform patterns considered in this example, the non-uniform FSDT reference models yield

$$\text{for } \{0.45, 0.15\}: \tilde{M}^T(z) = \frac{0.3186(z - 0.3808)\left(z^2 + 0.5384z + 0.1216\right)}{z^4 - 0.2183z^2 + 0.09072} = \frac{\alpha_M \tilde{\tilde{B}}_M^T(z)}{\left[A_M^{NT}\right]^T(z)} \tag{51}$$

$$\text{for } \{0.55, 0.05\}: \tilde{\tilde{M}}^T(z) = \frac{0.3536(z - 0.3625)\left(z^2 + 0.4050z + 0.0462\right)}{z^4 - 0.2183z^2 + 0.09072} = \frac{\alpha_M \tilde{\tilde{B}}_M^T(z)}{\left[A_M^{NT}\right]^T(z)} \tag{52}$$

A similar figure to Fig. 3 could be shown to check the accurateness of the non-uniform reference model according to each sampling pattern. For brevity, now it is not shown.

Design steps: Once every model is presented, the design of the RST control stage and the multi-rate controllers can be carried out.

Starting from the RST controller, solving (25) for the present example, the RST polynomials in (26), (28) take this form

$$\begin{aligned} \bar{T}^{NT}(z_N) &= \frac{1 + \bar{t}_1 + \bar{t}_2}{k(1+b)} z_2 = 1.471404 z_2 \\ \bar{S}^{NT}(z_N) &= 1.136755 z_2 - 0.286035 \\ \bar{R}^{NT}(z_N) &= z_2 - 0.069024 \end{aligned} \tag{53}$$

So, the RST control law in (22) will be

$$U^{NT}(z_N) = \left(\frac{1.471404 z_2}{z_2 - 0.069024}\right) R^{NT}(z_N) - \left(\frac{1.136755 z_2 - 0.286035}{z_2 - 0.069024}\right) \left[\tilde{\tilde{Y}}_{DR}^T\right]^{NT}(z_N) \tag{54}$$

Now, from the SSDT and FSDT models for the process and for the desired closed-loop function, the fast side of the multi-rate controller can be obtained

– for the uniform sampling case:

$$G_2^T(z) = \frac{\tilde{B}_M^T(z)}{\tilde{B}^T(z)} = \frac{0.2439(z - 0.3922)}{0.3289(z - 0.3919)} \frac{\left(z^2 + 0.9059z + 0.3012\right)}{\left(z^2 + 1.415z + 0.5488\right)} \approx \frac{0.7415\left(z^2 + 0.9059z + 0.3012\right)}{\left(z^2 + 1.415z + 0.5488\right)} \tag{55}$$

– for the non-uniform sampling case with $\{0.45, 0.15\}$:

$$\tilde{\tilde{G}}_2^T(z) = \frac{\alpha_M \tilde{\tilde{B}}_M^T(z)}{\alpha \tilde{\tilde{B}}^T(z)} = \frac{0.3186(z - 0.3808)\left(z^2 + 0.5384z + 0.1216\right)}{0.4877(z - 0.3945)\left(z^2 + 0.7542z + 0.2537\right)} \approx \frac{0.6532\left(z^2 + 0.5384z + 0.1216\right)}{\left(z^2 + 0.7542z + 0.2537\right)} \tag{56}$$

– for the non-uniform sampling case with $\{0.55, 0.05\}$:

$$\tilde{\tilde{G}}_2^T(z) = \frac{\alpha_M \tilde{\tilde{B}}_M^T(z)}{\alpha \tilde{\tilde{B}}^T(z)} = \frac{0.3536(z - 0.3625)\left(z^2 + 0.4050z + 0.0462\right)}{0.6144(z - 0.3795)\left(z^2 + 0.4630z + 0.0920\right)} \approx \frac{0.5755\left(z^2 + 0.4050z + 0.0462\right)}{\left(z^2 + 0.4630z + 0.0920\right)} \tag{57}$$

The slow side of the multi-rate controller is the same for every case:

$$G_1^{NT}(z_N) = \frac{B^{NT}(z_N)}{B_M^{NT}(z_N)} = \frac{0.6656(z_2 - 0.1092)}{0.3692(z_2 - 0.1138)} \approx 1.8028 \tag{58}$$

Note that, in both controller's sides, a cancellation between original zeroes of the process and of the reference model is considered (there are negligible differences due to the discretization method).

5.2. Stability analysis

From some of the previous expressions, the condition (41) can be evaluated for different situations. Seeing Fig. 3, Remark 4 can be assumed, and then, for the sake of simplicity, let us only focus on a uniform scenario in which a mismatch Δ between the model gain and the process gain appears. So, from (46), the real process $G_0^T(z) = \Delta G^T(z)$. Three different cases for Δ will be analyzed: $\Delta = 2$, 2.2, 2.3. The right hand in (41), $\left|1 + H_{lg}^{NT}(z_N)\right|$, does not depend on Δ, yielding these upper-bounds:

Table 1
Performance variation in LPTV scenarios.

	Performance variation $\|\|\pi(\tau_i) - \pi(\tau)\|\|$	
	$\left\|\left\|\pi\left(\left\{0.45, 0.15\right\}\right) - \pi(0.3)\right\|\right\|$	$\left\|\left\|\pi\left(\left\{0.55, 0.05\right\}\right) - \pi(0.3)\right\|\right\|$
Non-uniform case	0.0033	0.0023
Uniform case applied non-uniformly	0.0649	0.1208

– for $z_N = 1 \rightarrow 2.36$
– for $z_N = -1 \rightarrow 0.55$

But the left hand, $\left|H_{lg}^{NT}(z_N) - H_{lg,0}^{NT}(z_N)\right|$, does depend on Δ, resulting the next three cases:

– for $\Delta = 2$: $z_N = 1 \rightarrow 1.36$, and $z_N = -1 \rightarrow 0.44$. That is, (41) holds.
– for $\Delta = 2.2$: $z_N = 1 \rightarrow 1.63$, and $z_N = -1 \rightarrow 0.53$. That is, (41) holds but the control system is practically on the verge of instability (the value obtained for $z_N = -1$ is close to the upper-bound).
– for $\Delta = 2.3$: $z_N = 1 \rightarrow 1.77$, and $z_N = -1 \rightarrow 0.57$. That is, (41) does not hold (the value obtained for $z_N = -1$ is higher than the upper-bound), and hence the closed-loop response becomes unstable.

The reader can check that there exist negligible differences between the previous values and those obtained for a non-uniform model (as commented in Remark 4; details omitted for brevity). Figs. 4 and 5 show, respectively, the closed-loop outputs and control actions for each case compared to the nominal scenario ($\Delta = 1$, where no modeling errors are considered). The previous conclusions can be stated in these figures. As expected, the higher Δ is, the more degraded the control system performance will be.

Now, let us define the discrete-time control system performance π by means of the dominant closed-loop poles $z_N = \alpha \pm \beta j$. Then, $\pi \equiv \left\{\alpha \pm \beta j\right\}$. For a (non-uniform) LPTV control system, this performance will be represented by $\pi(\tau_i)$, $i = 1, 2, \ldots, N$, and it will be deduced from (38). If a uniform sampling case is treated, $\pi(\tau_i)$ will be replaced by $\pi(\tau)$, since every subperiod is equally time spaced. This last case will be named as the nominal, desired performance.

The goal is to compare the nominal performance with that performance obtained in two different non-uniform sampling situations:

a) When the uniform controller is used (despite the non-uniform actuation).

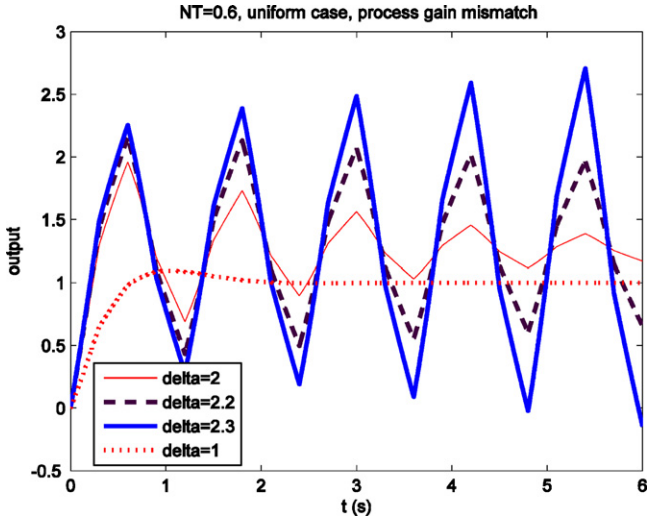

Fig. 4. Outputs for the uniform case with process gain mismatch.

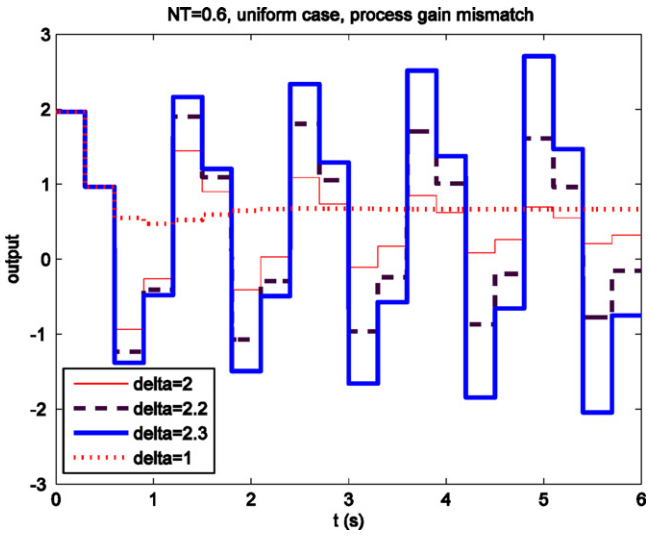

Fig. 5. Control actions for the uniform case with process gain mismatch.

b) When the suitable non-uniform controller is used (for each non-uniform pattern considered in the example, i.e. $\left\{0.45, 0.15\right\}$ and $\left\{0.55, 0.05\right\}$).

To achieve the comparison, the norm of the difference of the performance for a non-uniform sampling case and for the nominal case is calculated, that is, $\left\|\pi(\tau_i) - \pi(\tau)\right\|$. Table 1 shows the results. The variations on the performance are much lower (practically negligible) when, in a non-uniform context, the appropriate non-uniform controller is used. When using the uniform controller in a non-uniform sampling situation, some performance degradation is expected (the higher the first subperiod is, the more degradation will be expected).

The previous study has been developed assuming the non-uniform sampled-data system as a LPTV system. But, in a more realistic context, different non-uniform patterns are expected to be appeared. In this case, as switching among controllers is required, control system stability must be assessed. So, applying the LMIs in (44), a minimum α for which a feasible solution Q exists will be obtained. The decay rate guaranteed from the LMIs will be studied for two different situations: switching among non-uniform controllers, or using a unique uniform controller. Table 2 shows the results. A smaller decay rate is obtained when the switching among the different non-uniform controllers is carried out in a non-periodic situation. If a (unique) uniform controller is used in this context, the decay rate worsens around 18.5%.

Table 2
Decay rate for non-periodic scenarios.

	Decay rate α
Non-uniform case	0.303
Uniform case applied non-uniformly	0.358

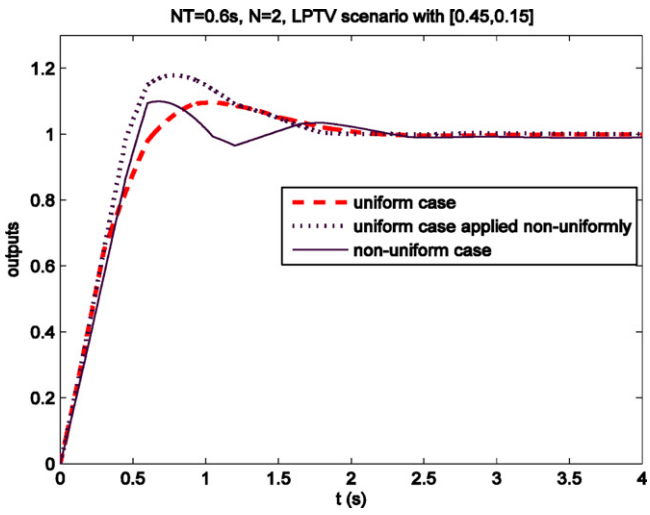

Fig. 6. Outputs for the LPTV scenario with {0.45, 0.15}.

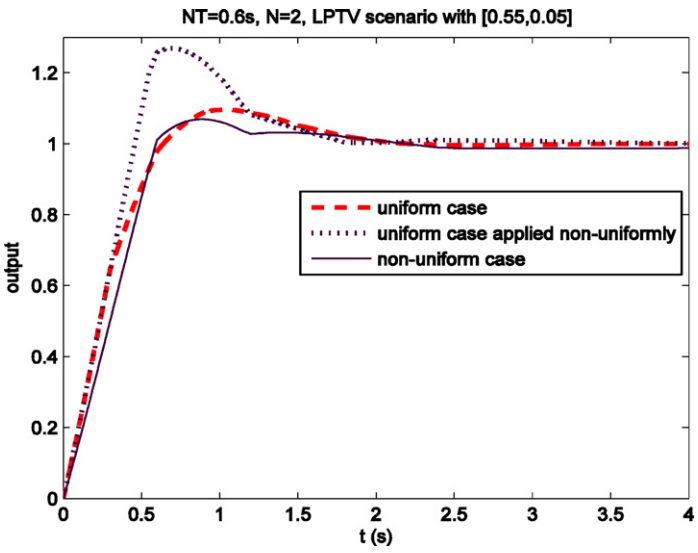

Fig. 8. Outputs for the LPTV scenario with {0.55, 0.05}.

5.3. Closed-loop outputs

Now, in order to better compare the different scenarios (since significant differences in overshoot can appear), closed-loop outputs are obtained. Fig. 6 shows the LPTV case when the pattern is $\{0.45, 0.15\}$. Focusing on overshoot and settling time, differences between the uniform, nominal output and the non-uniform one are practically negligible. Only the peak time for the latter response is a bit lower. However, considering a uniform controller in a non-uniform sampling context, its output shows some overshoot degradation (around 8%). This result confirms that one previously determined by the norm. In any case, as expected, ripple-free closed-loop responses to step reference signal are depicted. In Fig. 4, the control updating pattern can be observed (Fig. 7).

Similar conclusions can be deduced from Figs. 8 and 9, where the pattern $\{0.55, 0.05\}$ is simulated, but now a higher degradation in terms of overshoot (around 16%) is reflected for the uniform controller in a non-uniform sampling context (as expected according to Table 1).

Finally, the simulation of the non-periodic scenario is presented in Fig. 10. From inspection of this figure, if the switching between the two non-uniform controllers is carried out, the settling time is similar than in the uniform case, and the overshoot is clearly lower (a 6%). Nevertheless, if the uniform controller is used in the

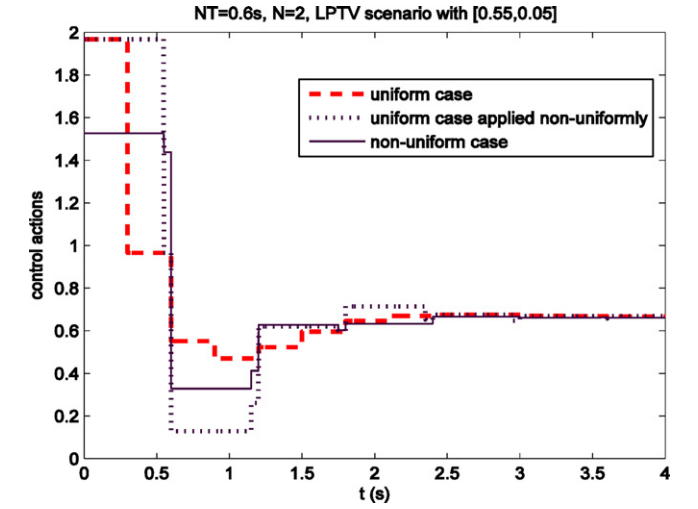

Fig. 9. Control actions for the LPTV scenario with {0.55, 0.05}.

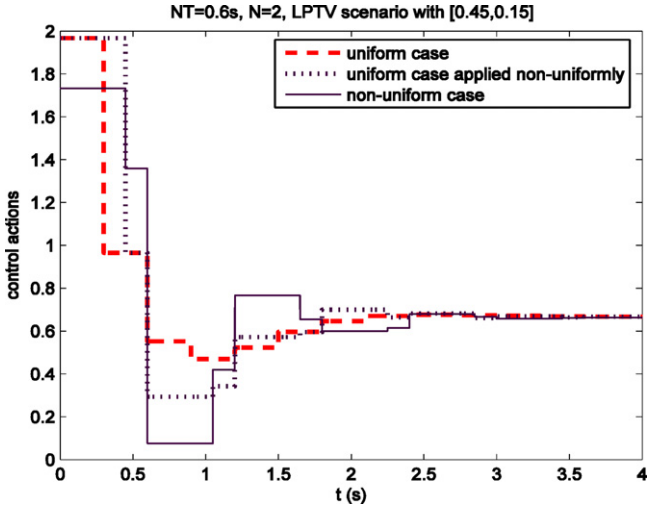

Fig. 7. Control actions for the LPTV scenario with {0.45, 0.15}.

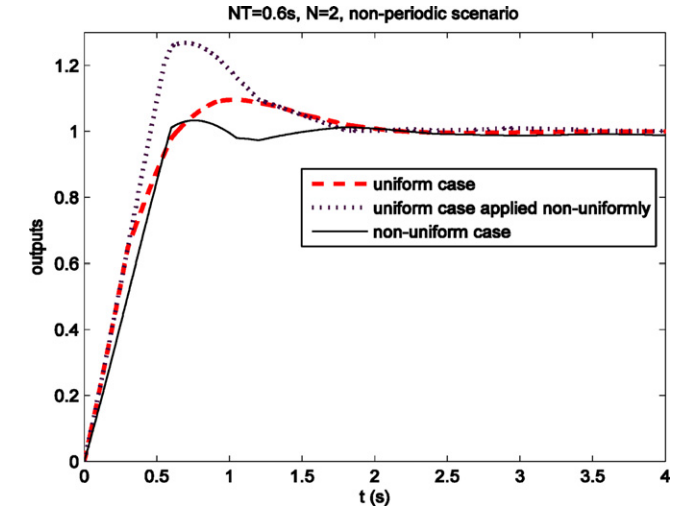

Fig. 10. Outputs for the non-periodic scenario.

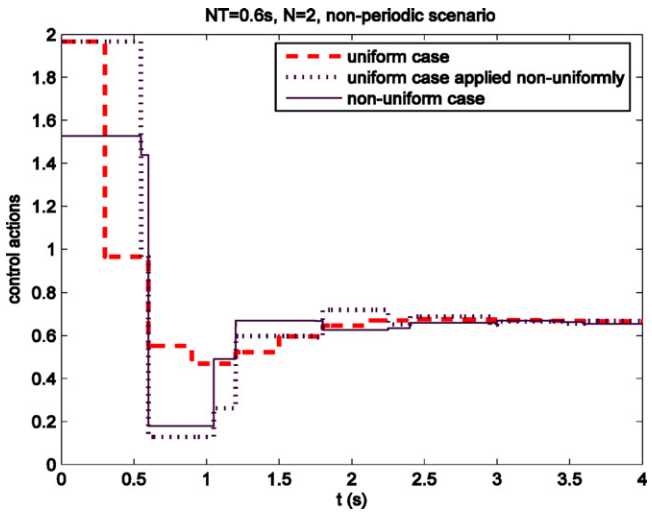

Fig. 11. Control actions for the non-periodic scenario.

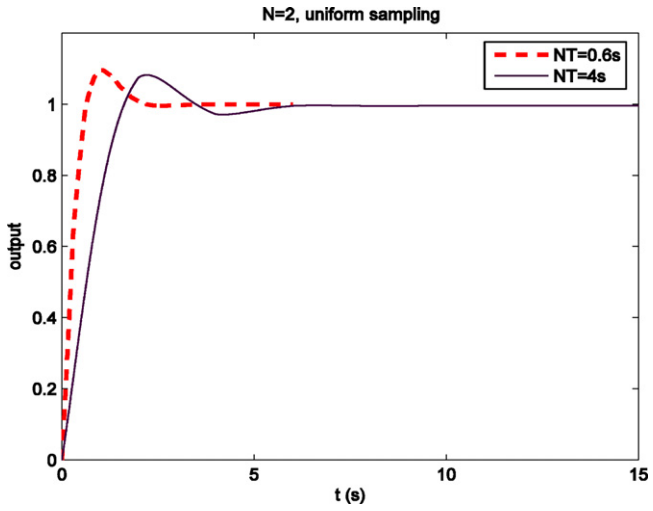

Fig. 12. Outputs for uniform scenarios at different process output sampling periods.

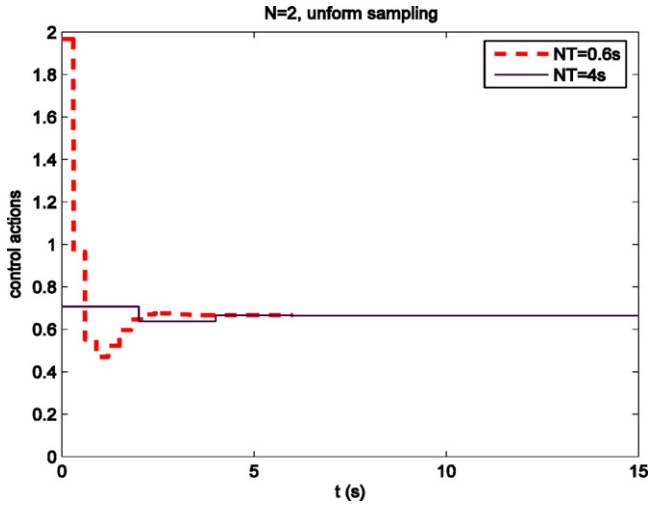

Fig. 13. Control actions for uniform scenarios at different process output sampling periods.

non-periodic context, the response worsens in terms of overshoot (around 15%). As assured by the LMIs, control system stability is preserved despite switching between controllers. Fig. 11 shows the non-uniform pattern alternation (firstly $\{0.55, 0.05\}$ is considered, and secondly $\{0.45, 0.15\}$; and so on cyclically).

5.4. A particular case

In slow dynamic processes, for example in chemical plants, the interval of quality sampling is often close to or even longer than the settling time of the process. In order to check if our design proposal is still applicable under this consideration (that is, if control performance and stability are preserved), the next case study is carried out.

Given the previous continuous time process $G(s)=(s+3)/(s^2+2s+2)$, which presents a settling time around 4 s ($t_s=4$ s). Now the output sampling period NT is taken as long as t_s (that is, $NT=4$ s, with $N=2$). The reference model is also the previous one, that is, $M(s)=(s+3)/(s^2+4s+8)$ (which presents $t_s=2$ s). For brevity, only the uniform sampling case is treated. Then, the next multi-rate controller including the RST stage is designed:

– RST stage

$$\begin{aligned}\bar{T}^{NT}(z_N) &= 0.7009 z_2 \\ \bar{S}^{NT}(z_N) &= -0.0192 z_2 - 0.00016 \\ \bar{R}^{NT}(z_N) &= z_2 + 0.0055\end{aligned} \tag{59}$$

– Fast side of the multi-rate controller:

$$G_2^T(z) \approx \frac{0.2481\left(z^2 - 0.02394z + 3.355\cdot 10^{-4}\right)}{\left(z^2 - 0.1126z + 0.01832\right)} \tag{60}$$

– Slow side of the multi-rate controller:

$$G_1^{NT}(z_N) \approx 4.0657 \tag{61}$$

In Fig. 12, the resultant control system output response is compared to that obtained when $NT=0.6$ s (shown in previous figures). As depicted, closed-loop stability is preserved, but control system performance decreases. Concretely, despite keeping the overshoot, the desired settling time ($t_s=2$ s) is not reached. The reason can be explained by Fig. 13, where control actions are shown. The control signal magnitude for this particular case is much lower than in the other case, which can reduce the convergence speed.

6. Conclusions

An approach to face the appearance of a sequence of different non-uniform sampling patterns in multi-rate sampled-data systems is introduced. This approach is based on including an RST control stage in the multi-rate control system. This inclusion simplifies the multi-rate controller design, which is model-based. The overall multi-rate control system is designed to avoid ripple closed-loop responses to step references.

To develop the design proposal, a suitable input/output modeling for non-uniform sampled-data systems is required. This modeling is based on the so-called non-uniform operator, which introduces some replacements for the classical, uniform z^{-i} operator. In this way, z^{-i} is able to represent the behavior of a non-uniformly sampled system.

As a non-periodic scenario is assumed, switching among multi-rate controllers will be needed. To assess stability in this situation, an LMI analysis must be carried out. Simulation results show how control system performance can be kept, and stability preserved, with this control strategy.

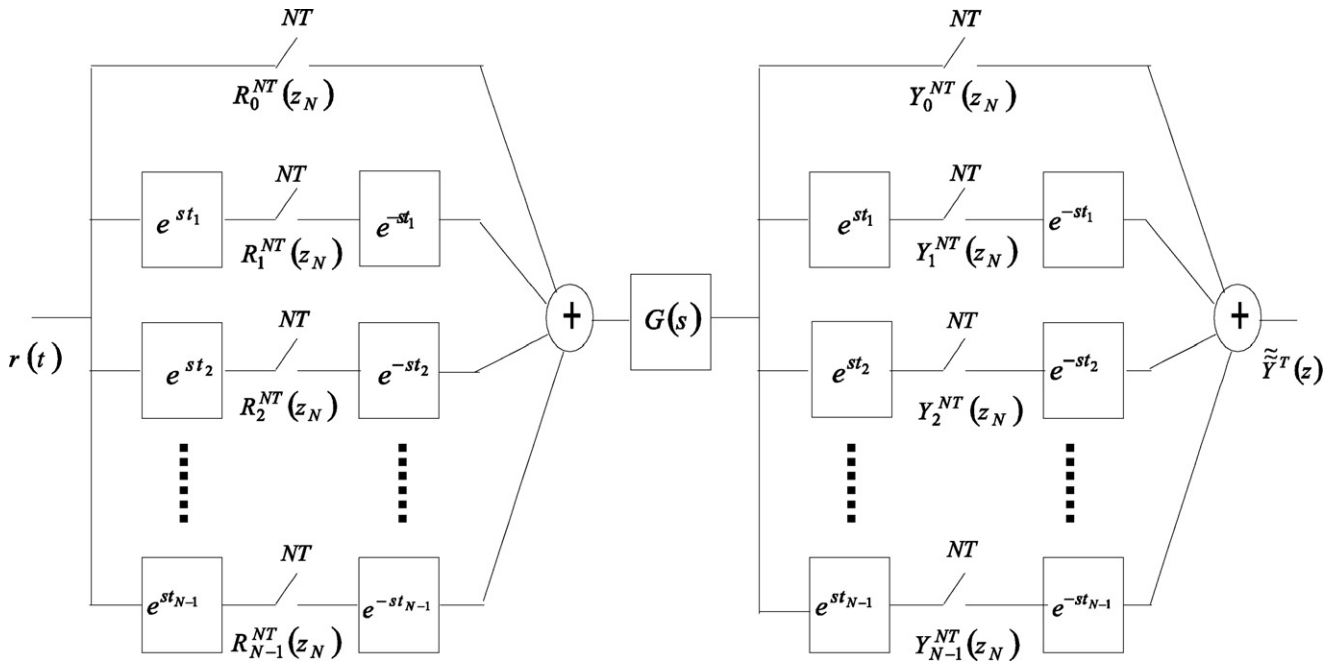

Fig. 14. Vector switch decomposition for the non-uniform sampling pattern.

Acknowledgments

The authors A. Cuenca and J. Salt are grateful to the Spanish Ministry of Education research Grants DPI2011-28507-C02-01 and DPI2009-14744-C03-03. In addition, A. Cuenca is grateful to Generalitat Valenciana Grant GV/2010/018, and J. Salt to the financial support of the Spanish Ministry of Education, "Salvador de Madariaga" Program PR2010-0310.

Appendix I.

Fig. 14 illustrates the vector switch decomposition [15] for a non-uniform sampling pattern, where input and output samplers are synchronized (remember Fig. 2). From this method, the aim is to find a representation for the non-uniformly sampled system.

As known, in a uniform scenario, the overall output sequence $Y^T(z)$ is obtained as

$$Y^T(z) = \sum_{m=0}^{N-1} z^{-m} Y_m^{NT}(z_N) \tag{62}$$

where z^{-m} is the uniform delay operator, and the m-th output sequence is calculated as

$$Y_m^{NT}(z_N) = \sum_{i=0}^{N-1} R_i^{NT}(z_N) G_{m-i}^{NT}(z_N) \tag{63}$$

where

- $R_i^{NT}(z_N) \triangleq Z_{NT}[R(s)e^{st_i}]$, that is, the Z-transform of the input sequence at NT-period advanced t_i time instants, and
- $G_{m-i}^{NT}(z_N) \triangleq Z_{NT}\left[H_{NT}(s)G_p(s)e^{s(t_m-t_i)}\right]$, that is, the Z-transform of the NT-period discretized impulse response, advanced t_m-t_i time instants.

But, in a non-uniform sampling scenario the z^{-m} delay operator cannot be used to represent the sampled process. In this case, to finally obtain the process description, first of all the sampled process output is needed to be defined in the Laplace domain. So, if the input $r(t) = e^{jwt}$ is considered, the output will yield

$$Y^*(s) = \frac{1}{NT}\left\{\sum_{m=0}^{N-1}\sum_{i=0}^{N-1} e^{jwt_i} G_{m-i}^{NT}(e^{jwNT}) e^{-st_m}\right\} \sum_{k=-\infty}^{\infty} \frac{1}{s - j(w + kw_0)} \tag{64}$$

where

- $Y^*(s)$ means Laplace transform of the sampled output,
- $w_0 = \frac{2\pi}{NT}$, $z_N = e^{jwNT}$, and
- e^{-st_m} is used to place each periodic output sequence in the corresponding time instant.

Letting $k = 0$ in order to eliminate sampling replicas, the gain of the process is given by

$$\begin{aligned} G_p^*(jw) &= \frac{1}{NT}\sum_{m=0}^{N-1}\sum_{i=0}^{N-1} e^{jwt_i} G_{m-i}^{NT}(e^{jwNT}) e^{-jwt_m} \\ &= \frac{1}{NT}\sum_{m=0}^{N-1}\sum_{i=0}^{N-1} G_{m-i}^{NT}(e^{jwNT}) e^{-jw(t_m-t_i)} \end{aligned} \tag{65}$$

(65) can be reorganized in this way

$$\begin{aligned} G_p^*(jw) = \frac{1}{NT}\sum_{i=0}^{N-1}\Bigg[&\sum_{m=0}^{i-1} G_{m-i}^{NT}(e^{jwNT}) e^{-jw(t_m-t_i)} \\ &+ \sum_{m=i}^{N-1} G_{m-i}^{NT}(e^{jwNT}) e^{-jw(t_m-t_i)}\Bigg] \end{aligned} \tag{66}$$

For the first term in (66), m-$i < 0$. As the next equation holds $G_{-k}^{NT}(e^{jwNT}) = e^{-jwNT} G_{N-k}^{NT}(e^{jwNT})$, then $G_p^*(jw)$ can be rewritten as

$$G_p^*(jw) = \frac{1}{NT}\sum_{i=0}^{N-1}\left[\sum_{m=0}^{i-1} e^{-jwNT} G_{N-(i-m)}^{NT}(e^{jwNT}) e^{-jw(t_m - t_i)} + \sum_{m=i}^{N-1} G_{m-i}^{NT}(e^{jwNT}) e^{-jw(t_m - t_i)}\right] \quad (67)$$

Now, in the first term in (67), let $N-(i-m)=x$, and in the second term let $m-i=x$. Then, (67) is rewritten as

$$G_p^*(jw) = \frac{1}{NT}\sum_{i=0}^{N-1}\left[\sum_{x=N-i}^{N-1} G_x^{NT}(e^{jwNT}) e^{-jw\left(NT + t_{x+i-N} - t_i\right)} + \sum_{x=0}^{N-i-1} G_x^{NT}(e^{jwNT}) e^{-jw\left(t_{x+i} - t_i\right)}\right] \quad (68)$$

Note that in the first term in (68) the part of the exponent $NT + t_{x+i-N} - t_i$ is equal to $t_N + t_{x+i-N} - t_i = t_{x+i} - t_i$, and hence it takes the same form than in the second term. Instead of writing this expression as time instants t_i, let us write it as subperiods τ_i. Then (68) is rewritten as

$$G_p^*(jw) = \frac{1}{NT}\sum_{i=0}^{N-1} G_i^{NT}(e^{jwNT}) \sum_{k=1}^{N} \exp\left(-jw \sum_{l=k}^{k+i-1} \tau_l\right) \quad (69)$$

where if $l > N$ then $\tau_l = \tau_{l-N}$.

Remembering (1) and (2), the relationship $z_N = z^N$ can be derived. As from (69) a FSDT model $\tilde{\tilde{G}}^T(z)$ will be defined, $G_i^{NT}\left(z^N\right)$ will be used instead of $G_i^{NT}(z_N)$.

References

[1] J. Nie, E. Sheh, R. Horowitz, Optimal $H\infty$ control for hard disk drives with an irregular sampling rate, in: Proceedings of the American Control Conference, 2011, pp. 5382–5387.

[2] P. Albertos, A. Crespo, Real-time control of non-uniformly sampled systems, Control Engineering Practice 7 (4) (1999) 445–458.

[3] A. Cuenca, J. Salt, P. Albertos, Implementation of algebraic controllers for non-conventional sampled-data systems, Real-Time Systems 35 (2007) 59–89.

[4] C. Lozoya, J. Romero, P. Martí, M. Velasco, J.M. Fuertes, Embedding Kalman techniques in the one-shot task model when non-uniform samples are corrupted by noise, in: Proceedings of the 18th Mediterranean Conference on Control and Automation, 2010, pp. 701–706.

[5] Y. Tipsuwan, M.-Y. Chow, Control methodologies in networked control systems, Control Engineering Practice 11 (2003) 1099–1111.

[6] J. Hespanha, P. Naghshtabrizi, Y. Xu, A survey of recent results in networked control systems, Proceedings of the IEEE 95 (1) (2007) 138–162.

[7] A. Sala, A. Cuenca, J. Salt, A retunable PID multi-rate controller for a networked control system, Information Science 179 (14) (2009) 2390–2402.

[8] K. Astrom, Event based control, in: Analysis and Design of Nonlinear Control Systems, 2007, pp. 127–147.

[9] H. Raghavan, A.K. Tangirala, R.B. Gopaluni, S.L. Shah, Identification of chemical processes with irregular output sampling, Control Engineering Practice 14 (2006) 467–480.

[10] D. Dasgupta, S.C. Patwardhan, NMPC of a continuous fermenter using Wiener–Hammerstein model developed from irregularly sampled multi-rate data, in: Proceedings of the 9th International Symposium on Dynamics and Control of Process Systems, 2010, pp. 623–628.

[11] M. Srinivasarao, S.C. Patwardhan, R.D. Gudi, Nonlinear predictive control of irregularly sampled multirate systems using blackbox observers, Journal of Process Control 17 (2007) 17–35.

[12] P. Khargonekar, K. Poolla, A. Tannenbaum, Robust control of linear time-invariant plants using periodic compensation, IEEE Transactions on Automatic Control 30 (11) (1985) 1088–1096.

[13] A. Cuenca, J. Salt, A. Sala, R. Pizá, A delay-dependent dual-rate PID controller over an Ethernet network, IEEE Transactions on Industrial Information 7 (2011) 18–29.

[14] A. Cuenca, P. García, P. Albertos, J. Salt, A non-uniform predictor-observer for a networked control system, International Journal of Control, Automation and Systems 9 (6) (2011) 1194–1202.

[15] G.M. Kranc, Input–output analysis of multirate feedback systems, IEEE Transactions on Automatic Control 3 (1957) 21–28.

[16] S.-C. Wu, M. Tomizuka, Performance and aliasing analysis of multi-rate digital controllers with interlacing, in: Proceedings of the American Control Conference, 2004, pp. 3514–3519.

[17] J. Salt, P. Albertos, Model-based multirate controllers design, IEEE Transactions on Control Systems Technology 13 (6) (2005) 988–997.

[18] M. Cimino, P.R. Pagilla, Design of linear time-invariant controllers for multirate systems, Automatica 46 (2010) 1315–1319.

[19] M. Cimino, P.R. Pagilla, Input-state model matching and ripple-free response for dual-rate systems, Systems & Control Letters 60 (2011) 815–824.

[20] M. Cimino, P.R. Pagilla, Conditions for the ripple-free response of multirate systems using linear time-invariant controllers, Systems & Control Letters 59 (2010) 510–516.

[21] L. Xie, Y.J. Liu, H.Z. Yang, F. Ding, Modelling and identification for non-uniformly periodically sampled-data systems, IET Control Theory Applications 4 (5) (2010) 784–794.

[22] E.K. Larsson, M. Mossberg, T. Soderstrom, Identification of continuous-time ARX models from irregularly sampled data, IEEE Transactions on Automatic Control 52 (3) (2007) 417–427.

[23] W.H. Li, S.L. Shah, D.Y. Xiao, Kalman filters in non-uniformly sampled multirate systems: for FDI and beyond, Automatica 44 (1) (2008) 199–208.

[24] A.K. Tangirala, D. Li, R.S. Patwardhan, S.L. Shah, T. Chen, Ripple-free conditions for lifted multirate control systems, Automatica 37 (10) (2001) 1637–1645.

[25] T. Coffey, I. Williams, Stability analysis of multiloop, multirate sampled systems, AIAA Journal 4 (1966) 2178–2190.

[26] K.J. Astrom, B. Wittenmark, Computer-Controlled Systems: Theory and Design, Prentice Hall, 1984.

[27] D. Liberzon, A.S. Morse, Basic problems in stability and design of switched systems, IEEE Control Systems Magazine 19 (5) (1999) 59–70.

[28] H.W. Thomas, N.P. Lutte, Z-transform analysis of nonuniformly sampled digital filters, Proceedings of the IEE 119 (11) (1972) 1559–1567.

[29] J. Salt, A. Sala, P. Albertos, A transfer-function approach to dual-rate controller design for unstable and non-minimum-phase plants, IEEE Transactions on Control Systems Technology 19 (5) (2011) 1186–1194.

[30] S. Boyd, L. El Ghaoui, E. Feron, V. Balakrishnan, Linear matrix inequalities in system and control theory, Society for Industrial Mathematics (1994).

[31] A. Sala, Computer control under time-varying sampling period: an LMI gridding approach, Automatica 41 (12) (2005) 2077–2082.